Scaling range and cutoffs in empirical fractals

Ofer Malcai,* Daniel A. Lidar,[†] and Ofer Biham[‡]

Racah Institute of Physics, The Hebrew University, Jerusalem 91904, Israel

David Avnir[§]

Institute of Chemistry and the Minerva Center for Computational Quantum Chemistry, The Hebrew University, Jerusalem 91 904, Israel

Fractal structures appear in a vast range of physical systems. A literature survey including *all experimental papers on fractals* which appeared in the six Physical Review journals (A–E and Letters) during the 1990s shows that experimental reports of fractal behavior are typically based on a scaling range Δ that spans only 0.5–2 decades. This range is limited by upper and lower cutoffs either because further data are not accessible or due to crossover bends. Focusing on spatial fractals, a classification is proposed into (a) aggregation, (b) porous media, (c) surfaces and fronts, (d) fracture, and (e) critical phenomena. Most of these systems [except for class (e)] involve processes far from thermal equilibrium. The fact that for self-similar fractals [in contrast to the self-affine fractals of class (c)] there are hardly any exceptions to the finding of $\Delta \lesssim 2$ decades, raises the possibility that the cutoffs are due to intrinsic properties of the measured systems rather than the specific experimental conditions and apparatus. To examine the origin of the limited range we focus on a class of aggregation systems. In these systems a molecular beam is deposited on a surface, giving rise to nucleation and growth of diffusion-limited-aggregation-like clusters. Scaling arguments are used to show that the required duration of the deposition experiment increases exponentially with Δ. Furthermore, using realistic parameters for surfaces such as Al(111) it is shown that these considerations limit the range of fractal behavior to less than two decades in agreement with the experimental findings. It is conjectured that related kinetic mechanisms that limit the scaling range are common in other nonequilibrium processes that generate spatial fractals. [S1063-651X(97)13609-1]

PACS number(s): 64.60.Ak, 61.43.Hv, 82.20.Mj, 68.55.−a

I. INTRODUCTION

The concept of fractal geometry [1,2] has proved useful in describing structures and processes in experimental systems [3–9]. It provides a framework that can quantify the structural complexity of a vast range of physical phenomena. Fractals are objects that exhibit similar structures over a range of length scales for which one can define a noninteger dimension. There are different procedures to evaluate the fractal dimension of an empirical fractal, all based on multiple resolution analysis. In this analysis one measures a property P of the system (such as mass, volume, etc.) as a function of the resolution used in measuring it (given by a yardstick of linear size r). Fractal objects are characterized by

$$P = kr^{-D}, \tag{1.1}$$

where D is the fractal dimension and k is a prefactor (related to the lacunarity of the object). For such objects the graph of

log$_{10}P$ versus log$_{10}r$ exhibits a straight line over a range of length scales $r_0 < r < r_1$ where r_0 (r_1) is the lower (upper) cutoff. The fractal dimension D is given by the slope of the line within this range. Typically, the range of linear behavior terminates on both sides by r_0 and r_1 either because further data are not accessible or due to crossover bends beyond which the slope changes. For example, in spatial fractals the scaling range is limited from below by the size of the basic building blocks from which the system is composed and from above by the system size. However, the empirically measured scaling range may be further reduced due either to properties of the measured system or limitations of the apparatus. System properties that may further restrict the scaling range may be (a) mechanical strength of the object which is reduced with increasing size, (b) processes that tend to smooth out the structure and compete with the fractal generating processes, (c) noise, impurities, and other imperfections in the system, and (d) depletion of resources such as space available for growth or feed material. The apparatus may limit the observed scaling range due to (a) limited resolution at the smallest scales, (b) limited scanning area, which may be smaller than the system size, (c) limited speed of operation, which does not allow one to collect enough statistics, (d) constraints in operation conditions such as temperature, pressure, etc., which may impose parameters not ideal for the given experiment.

There are different ways to classify empirical fractals. One classification is according to the type of space in which they appear. This can be (a) real space, (b) phase space, (c) parameter space, and (d) the time domain (time series). Spa-

tial fractals appear in both equilibrium and nonequilibrium systems. The theory of critical phenomena predicts that at the critical point of fluids, magnets, and percolation systems the correlation length diverges [10,11]. As a result, fractal domain structures appear over all length scales up to the system size. Experimental evidence for fractal structures at criticality has been obtained for example, in the context of percolation [12], in agreement with the theory [13,14] and computer simulations [15,16]. Reaching the critical point requires fine tuning of the system parameters, as *these points are a set of measure zero in parameter space*. Most empirical fractals have been found in systems far from thermal equilibrium and thus not only out of the scope of critical phenomena, but where equilibrium statistical physics does not apply.

A variety of dissipative dynamical systems exhibit strange attractors with fractal structures in phase space. The theory of dynamical systems provides a theoretical framework for the study of fractals in such systems at the transition to chaos and in the chaotic regime [17]. At the transition to chaos, fractals are found also in parameter space [18] while time series measured in the chaotic regime exhibit fractal behavior in the time domain [19]. Fractal dimensions of objects in phase space are not limited by the space dimension, giving rise to the possibility of $D > 3$. Effective methods for embedding experimental time series in higher dimensional spaces to examine the convergence of fractal dimension calculations were developed and widely applied [20]. However, these should be used with care as the number of data points required in order to measure fractal dimensions (FD) from embedded time series increases exponentially with the dimension of the underlying attractor [21].

In this paper we will focus on fractals in real space. One can classify the spatial fractal structures according to physical processes and systems in which they appear. We identify the following major classes: (a) aggregation, (b) porous media, (c) surfaces and fronts, (d) fracture, (e) critical phenomena (e.g., in magnets, fluids, percolation). Note that some systems may belong to more than one class. For example, classes (a) and (d) describe the dynamical processes that generate the fractal while classes (b) and (c) describe the structure itself. Moreover, there is some overlap between (b) and (c) since studies of porous media often focus on the fractal structure of the internal surfaces of the pores [22]. For case (e) of equilibrium critical phenomena there are solid theoretical predictions of fractal structures at the critical point, most extensively examined for the case of percolation [13,14]. The cutoffs in such systems may appear due to small deviations of the parameters from the critical point values and due to the finite system size. Spatial fractals in the four other classes typically result from nonequilibrium processes. One should single out the case of surfaces and fronts (c), which are often inherently anisotropic and their fractal nature is characterized by self-affine rather than self-similar structure [9]. Among the other three classes, within the physics literature, fractals in aggregation phenomena have been most extensively studied.

The abundance of fractals in aggregation processes stimulated much theoretical work in recent years. The diffusion-limited-aggregation (DLA) model, introduced by Witten and Sander [23,24], provides much useful insight into fractal growth [25]. This model includes a single cluster to which additional particles attach once they reach a site adjacent to the edge of the cluster. The additional particles are launched one at a time from random positions far away from the cluster and move as random walkers until they either attach to the cluster or move out of the finite system. Numerical simulations of this model were used to create very large fractal clusters of up to about 30×10^6 particles [26]. These clusters exhibit fractal behavior over many orders of magnitude (although the lacunarity seems to change as a function of the cluster size). The asymptotic behavior of the DLA cluster has been studied analytically and numerically for both lattice and continuum models, indicating a considerable degree of universal behavior [27,28]. A universal fractal dimension $D \cong 1.7$ was observed in two dimensions (2D) and $D \cong 2.5$ in three dimensions (3D) [29].

Morphologies similar to those of the DLA model and fractal dimensions around 1.7 have been observed in a large number of distinct experimental systems. These include electrodeposition [30] and molecular beam epitaxy (MBE) [31]. However, unlike the theoretical model, the experimentally observed morphologies are typically somewhat more compact and the scaling range does not exceed two orders of magnitude. This observation has to do with the fact that unlike theoretical models, which may be inherently scale free, in empirically observed fractals the range of length scales over which scaling behavior is found is limited by upper and lower cutoffs. For finite systems, the scaling range is limited by lower and upper cutoffs even if the internal structure is scale free. In this case the lower cutoff is the basic unit (or atom) size in the system, while the upper cutoff is of the order of the system size. However, typically the scaling range is much narrower than allowed by the system size, thus limited by other factors. This width is not predicted by theoretical models and in many cases not well understood. There have been some suggestions on how to incorporate the limited range into the analysis procedure [32]. On the one hand, this range may be simply limited by the apparatus used in a given experiment. If this is the case, we would expect to see, at least in some experiments, when the most proper apparatus is chosen, a broad scaling range limited only by the system size. On the other hand, the scaling range may be limited by properties intrinsic to the system. In this case, using a different apparatus is not expected to dramatically broaden the scaling range.

In this paper we explore the status of experimental measurements of fractals. Using an extensive survey of experimental fractal measurements we examine the range of scales in which the fractal behavior is observed and the fractal dimensions obtained. We observe a broad distribution of measured dimensions in the range $0.5 < D < 3$, most of which are interpreted as nonuniversal dimensions, that depend on system parameters. This distribution includes a peak around $D = 1.7$ due to structures that resemble 2D DLA-like clusters, which account for a significant fraction of the class of aggregation processes. More importantly, we find that the range of fractal behavior in experiments is limited between 0.5–2 decades with very few exceptions as discussed above. There may be many different reasons for this, which can be specific to each system or apparatus. However, the fact that the distribution is sharply concentrated around 1.5 decades and the

remarkably small number of exceptions indicate that there may be some general common features that limit this range. Trying to identify such features, we focus in this paper on a class of aggregation problems that appear in MBE experiments. In these experiments a finite density of DLA-like clusters nucleate and grow on the substrate. The width of the scaling range is limited by the cluster size (upper cutoff), and the width of its narrow arms (lower cutoff) which can be as small as the single atom. We show that a small increase in the scaling range requires a large increase in the duration of the MBE experiments. Moreover, at long times edge diffusion and related processes that tend to smooth out the fractal structures become significant. These processes tend to increase the lower cutoff and in this way limit the possibility of further extending the scaling range. This detailed argument is presented only for MBE-like aggregation problems. However, we believe that related arguments, based on the fact that in empirical systems there is no complete separation of time scales, may apply to other classes of fractal structures out of equilibrium.

This paper is organized as follows. In Sec. II we present an extensive survey of experimental measurements of fractals and examine the empirical dimensions and scaling range. In order to obtain a better understanding of the limited scaling range, we focus in Sec. III on the case of nucleation and growth of fractal islands on surfaces. The width of the scaling range is obtained as a function of the parameters of the system and it is shown that under realistic assumptions it does not exceed two decades. These results and their implications to empirical systems are discussed in Sec. IV, followed by a summary in Sec. V.

II. SURVEY OF EXPERIMENTAL RESULTS

Here we present an extensive survey of experimental papers reporting fractal measurements, and examine the range of length scales over which fractal properties were observed, as well as the reported dimensions. In our survey we used the INSPEC database from which we extracted all the *experimental* papers in Physical Review A–E and Physical Review Letters over a period of seven years (January 1990– December 1996) that include the word *fractal* in the title or in the abstract, a total of 165 papers [33]. These papers account for 9.1% of the 1821 experimental papers on fractals that appeared during that seven year period [and 6.8% of all such papers ever published (2425 papers since 1978)] in all scientific journals listed by INSPEC.

Experimental measurements of fractal dimensions are usually analyzed using the box counting or related methods. In these measurements a log-log plot is reported in which the horizontal axis represents the length scale (such as the linear box size) and the vertical axis is some feature (such as the number of boxes that intersect the fractal set) for the given box size. Typically, the reported curves include a range of linear behavior. This range terminates on both sides by upper and lower cutoffs either because further data are not accessible or due to a knee beyond which the line is curved. The apparent fractal dimension is then obtained from the slope of the line in the linear range. Out of the 165 papers mentioned above, 86 papers [34–119] included such a plot (and 10 of them included two plots). For each one of these 96 log-log

plots we extracted both the fractal dimension and the width of the linear range between the cutoffs (Table I) [120]. Table I includes a row for each one of the 96 measurements. The first column briefly describes the context of the experiment. The second column provides a classification of the systems into the following categories: aggregation (A), porous media (P), surfaces and fronts (S), fracture (F), critical phenomena (C), fracton vibrations (V), turbulence (T), random walk (R), and high energy physics (H). In cases where more than one class is appropriate we assign both classes. The next two columns provide the fractal dimension (FD) and the width of the scaling range in which fractal behavior was detected (Δ). The next three columns provide the lower cutoff (r_0), the upper cutoff (r_1), and the units in which these cutoffs are measured. Note that in many of the papers the scales in the log-log plots are provided in a dimensionless form or in arbitrary units. In these cases we left the units column empty. The last two columns provide the reference number and the figure number in that paper from which the FD, Δ, and the cutoffs were obtained. We found that 29 measurements belong to class A, 19 to P, 18 to S, 6 to F, 8 to C, 4 to V, 2 to T, 4 to R, and 10 to H.

To examine the distribution of widths of the scaling range we present a histogram (Fig. 1) that shows, as a function of the width (in decades) the number of experimental measurements in which a given range of widths was obtained. Surprisingly, it is found that the typical range is between 0.5 and 2 decades with very few exceptions. To obtain more insight about the scaling range we present separate histograms for aggregation [Fig. 2(a)], porous media [Fig. 2(b)], and surfaces and fronts [Fig. 2(c)]. The distribution for aggregation systems is basically similar to the one of Fig. 1, with a peak around 1.5 decades. We note in particular that it does not include measurements over significantly more than two decades. The width distribution for porous media has the same general shape, however, the scaling range is typically narrower and the peak is centered around one decade. The width distribution for surfaces and fronts includes both a flat range between one and two decades, in addition to a few cases with three and four decades. It is interesting to note that the papers in which three or four decades of scaling behavior are reported [46,72,87,90] are in the context of surfaces and fronts, related to self-affine, rather than self-similar fractals. This observation raises the question of whether, for self-similar fractals, there are some common features of the empirical systems reviewed here, which tend to limit the width of the scaling range.

To obtain the distribution of measured fractal dimensions we constructed a histogram (Fig. 3) showing the number of experiments that observed fractal dimension in a given range. The fact that most of the experiments deal with spatial fractals is reflected in the observation that in most cases $D \lesssim 3$ [121]. Two peaks are identified in the histogram, around $D \cong 1.7$ and $D \cong 2.5$. In addition to these peaks, there is a broad distribution of observed dimensions in the entire range of $0.5 < D < 3.0$. To further examine the observed dimensions we also show separately their distributions for the classes of aggregation [Fig. 4(a)], porous media [Fig. 4(b)] and surfaces [Fig. 4(c)]. The statistics available for the other classes is not sufficient to draw significant conclusions. We observe that for aggregation systems there is a huge peak

TABLE I. Experimental reports on fractals in Physical Review journals from January 1990 to December 1996, presented in chronological order. In the first column the context of each experiment is briefly mentioned. It is then classified, in the second column according to the following classification: aggregation (A); porous media (P); surfaces and fronts (S); fracture (F); critical phenomena (C); fracton vibrations (V); turbulence (T); random walk (R), and high energy physics (H). The next two columns provide the fractal dimension (FD) and the width of the scaling range in which fractal behavior was detected (Δ). The next three columns provide the lower cutoff (r_0), the upper cutoff (r_1), and the units in which these cutoffs are measured. For papers in which the log-log scales are provided in a dimensionless form or arbitrary units we left the units' column empty. The last two columns provide the reference number and the figure number in that paper from which the FD, Δ, and the cutoffs were obtained.

Experiment	Class	FD	Δ	r_0	r_1	Units	Ref.	Fig.
Aggregation of interacting colloidal gold particles	A	1.9	1.0	0.23	2.3	Å^{-1}	[34]	2
Elastic properties of colloidal gels	A,P	2.0	1.0	0.23×10^{-3}	2.5×10^{-3}	Å^{-1}	[35]	8
Low frequency dynamics in superionic borate glasses	V	3.3	0.7	1.6	8.0	cm^{-1}	[36]	7(a)
Fluctuations in granular ceramic superconductors	C	2.3	1.5	0.027	0.85		[37]	2
Role of local latent heat in Ge pattern formation	A	1.7	0.7	5.7	28.5		[38]	5
FD in silica aerogel - crystallized	P	2.8	0.8	0.8	5.2	nm	[39]	2
FD in silica aerogel - aerojel	P	2.3	1.1	0.13	1.8	nm^{-1}		3
Vibrational dynamics in silica aerogels	V	2.4	0.9	0.015	0.13	Å^{-1}	[40]	1
Conformation of graphite oxide membranes in solution	S	2.4	0.9	2.6	22	μm^{-1}	[41]	3
Viscous fingering in inhomogeneous porous models	S	1.5	1.3	2.15	40		[42]	11
Self-avoiding fractals: open magnetic chains in Fe-Cu	R	1.3	1.7	3	148		[43]	2(d)
Self-avoiding fractals: closed defect loops in Ni-Mo	R	1.2	1.1	0.023	0.31			5(b)
Fractal structure of cross-linked polymer resin	P	2.0	0.7	0.009	0.05	Å^{-1}	[44]	1
Diffusion-limited-aggregation-like structures in solids	A	1.7	1.7	2.6	120		[45]	3(a)
Gravity invasion percolation in 2D porous media	S	1.3	2.8	0.05	32		[46]	3
Isoscalar surfaces in turbulence	S	1.7	1.3	5.4	100		[47]	1
Viscous fingering in colloidal fluids	S	1.6	1.8	1	70		[48]	1(a)
Viscoelastic fracturing in colloidal fluids	F	1.4	1.8	1	70			1(c)
2D islands of Au on Ru(0001) (STM)	A	1.7	1.6	35	1500	Å	[49]	4(a)
Hyperscaling law on polymer clusters	C	2.5	1.0	0.01	0.1	Å^{-1}	[50]	1
Structure of silica gels [light scattering(LS)]	P	2.1	1.3	1.2×10^{4}	2.3×10^{5}	cm^{-1}	[51]	1
Morphology of polystyrene colloids (LS)	A	2.0	0.9	4.3×10^{-4}	3.3×10^{-3}	cm	[52]	6
Morphology of polystyrene colloids	A	1.6	1.1	8.5×10^{-4}	0.01	cm		7
Aggregation of colloidal particles at a liquid surface	A	1.5	1.6	3.16	112		[53]	4
Colloidal aggregation at the liquid-air interface	A	1.6	1.4	1.12	25.1		[54]	4(b)
Micrograph of Charpy fracture surface	F	1.2	1.9	2.5×10^{-3}	0.22	mm	[55]	3
Low-cycle-fatigue fracture surface	F	1.4	1.4	2.7×10^{-3}	0.07	mm		5
Patterns formed by laser in GeAl thin multilayer films	P	1.9	1.5	2	66		[56]	2
Particle production in hadron-nucleus interactions	H	0.8	1.0	1.0	10		[57]	3
Aggregation in a solution of polystyrene spheres (LS)	A	1.7	0.7	600	3000	cm^{-1}	[58]	4
Aggregation of self-assembled monolayer	A	1.7	1.8	10	600	nm	[59]	4(a)
Infinite percolation cluster in thin films	C	1.9	1.3	1.41	26.6		[60]	4(a)
Fractal dimension of fractured surface	F	1.5	1.3	7.5	150	μm	[61]	1
Self affine growth of copper electrodeposits (STM)	S	2.5	1.5	10^{-4}	3×10^{-3}	nm^{-1}	[62]	3
Growth of fractal clusters on thin solid films	A	1.7	0.9	7.0	60		[63]	3(a)
Correlations in colloidal silica aerogels	P	1.6	0.9	0.3	2.4		[64]	4(b)
Correlations in colloidal silica aerogels	P	0.9	0.6	0.7	2.8			4(c)
Fractal electrodeposits of silver and copper films	A	1.5	1.4	1.0	23		[65]	2(c)
Multifractal analysis of nucleus-nucleus interactions	H	1.0	1.0	1.0	10		[66]	2
Period-doubling scenarios in Taylor-Couette flow	T	2.4	1.4	2.0	45		[67]	9(a)
2D aggregation of polystyrene latex particles (optical)	A	1.5	1.8	0.56	31.6		[68]	2
Nucleation-limited aggregation in aqueous-solution films (STM)	A	1.8	1.6	5.0	220		[69]	1(b)
Fractal electrodeposits grown under damped free convection	A	2.5	1.2	0.06	0.87	cm	[70]	3(a)
Colloidal aggregation induced by alternating electric fields	A	1.5	1.4	1.8	42	μm	[71]	2(b)
Fractal electrodes and interfaces	S	2.4	3.8	10	6×10^{4}	Hz	[72]	13
Fractal distribution of earthquake hypocenters	F	1.8	1.4	5.0	120	km	[73]	3

TABLE I. (*Continued*).

Experiment	Class	FD	Δ	r_0	r_1	Units	Ref.	Fig.
Pore space correlations in capillary condensation (LS)	P	2.6	1.4	0.1	2.5	μm^{-1}	[74]	3
Water desorption and adsorption in porous materials	P	1.7	0.8	0.02	0.14	$Å^{-1}$	[75]	3
Spin-lattice relaxation by paramagnetic dopants in $Li_2Si_2O_5$	C	3.0	1.3	0.5	10	s	[76]	5
Spin-lattice relaxation by paramagnetic dopants in $Na_2Si_2O_5$	C	2.1	1.3	0.5	10	s		5
Interface thickness in block copolymers	S	2.5	0.9	0.03	0.25	$Å^{-1}$	[77]	8(a)
Long range correlations in Silica aerogels	A,P	1.7	1.1	0.015	0.2	$Å^{-1}$	[78]	10
Low-frequency vibrational states in As_2S_3 glass	V	2.4	0.4	14	32	cm^{-1}	[79]	3
Heavily irradiated pure and doped NaCl crystals (Raman)	P	2.5	1.2	6	100	cm^{-1}	[80]	1
Multihadron production in high energy interactions	H	0.9	1.0	1.0	10		[81]	2
Pseudorapidity distribution for particles produced in pp collisions.	H	1.0	1.3	0.5	10		[82]	2
Multifractal moments in 800 GeV proton-nucleus interactions	H	0.7	1.7	0.2	9		[83]	1(a)
Electrodeposition of a gold oxide layer on a gold cathode (STM)	S	2.2	1.5	40	1258	Å	[84]	4(a)
Aggregation of 2D polystyrene particles (in-situ microscopy)	A	1.8	1.3	10	220	μm	[85]	3(d)
Fractal scaling behavior of vapor-deposited silver films	S	2.4	0.6	40	150		[86]	3
Tracer dispersion fronts in porous media (computer imaging)	S	1.4	2.5	0.1	32		[87]	5
Teritary structure of proteins	R	1.6	1.3	50	1000		[88]	1
Dense colloid silica suspensions in a H_2O-D_2O medium	P	1.6	0.4	0.9	2.5		[89]	2
2D aluminum corrosion fronts	S	1.2	3.7	2.0	10^4	μm	[90]	4
Aggregation of polystyrene latices (LS)	A	1.7	0.8	100	600	nm	[91]	4(a)
Aggregation of polystyrene latices (LS)	A	2.7	0.5	200	630	nm		4(c)
Diffusion of aggregates in carbonaceous flame soot aerosol (LS)	A,P	2.2	0.4	2.0	5.0		[92]	2
Spinodal decomposition in hydrogen-bonded polymer	A	2.4	0.4	5.6×10^{-3}	15×10^{-3}		[93]	3(a)
Broadband edge density fluctuations in compact helical system	T	6.0	2.0	100	10^4		[94]	3(a)
Graphitic oxide sheets suspended in aqueous solution	F	2.1	1.1	2.0	25	μm^{-1}	[95]	2
Structural analysis of electroless deposits	A	1.6	1.3	0.05	1.0		[96]	5(b)
Boson peak in the raman spectra of amorphous GaAs	V	2.5	0.6	300	1200	cm^{-1}	[97]	5
Fractal structure of porous solides characterized by adsorption	P	2.6	0.4	5.6	12.6		[98]	1(b)
Cold deposited silver flms determined by low temperature STM	S	2.5	1.8	0.03	2.0	nm^{-1}	[99]	6(a)
Porous glass characterized by adsorbed dibromomethane	P	2.3	0.7	0.03	0.15	$Å^{-1}$	[100]	3
Multifractality of medium energy particles in p-AgBr interactions	H	0.7	0.6	1.22	4.95		[101]	2(a)
Multifractality in proton-nucleus interaction	H	0.9	1.3	2	44		[102]	3
Multiplicity distributions from central collisions $^{16}O+Cu$	H	1.0	1.0	1.0	10		[103]	8(a)
Fractal analysis of the multiparticle production process	H	0.8	1.0	4.0	40		[104]	7
Double layer relaxation at rough electrodes	A	2.5	0.5	0.3	1.0	μA	[105]	2
Long range correlations in DNA sequences from wavelet analysis	R	1.0	2.4	16	4100		[106]	2
Percolation in a 3D disordered conductor insulator composite	C	1.9	0.8	0.1	0.6	μm	[107]	3
Percolation in a 3D disordered conductor insulator composite	C	2.6	0.5	0.6	2.0	μm		3
Oxide aggregation on liquid-gallium surface	A	1.5	2.1	0.45	55	μm	[108]	4
Dense branching morphology in Bi/Al/Mn/SiO films	S	1.6	2.0	9×10^{-3}	1.0		[109]	11(a)
Evolution of source rocks during hydrocarbon generation	P	2.5	1.6	5×10^{-3}	0.2	$Å^{-1}$	[110]	4(b)

TABLE I. (*Continued*).

Experiment	Class	FD	Δ	r_0	r_1	Units	Ref.	Fig.
Fractal dimension of Li insertion electrodes	S	2.3	2.0	5.0	500	mV/s	[111]	2 C
Cyclic I-V studies of In oxide films	S	1.8	2.3	1.0	200	mV/s	[112]	2
Sn oxyfluoride	S	1.9	1.2	1.5	23	μm		4
Intermittency in ^{197}Au fragmentation	H	1.0	1.3	2.0	40		[113]	4(a)
Evaporatively controlled growth of salt trees	A	2.3	0.8	0.25	1.6	cm	[114]	4(a)
Fractal growth during annealing of aluminum on silica	A	1.7	2.3	1.0	200		[115]	5
Flow of water pumped through pore space (NMR)	P,C	1.8	0.5	1.0	3.5		[116]	7(a)
Formation of side branches of xenon dendrites	S	1.4	2.4	0.015	4.0	mm	[117]	11
Aggregation of porphyrins in aqueous solutions	A	2.5	1.7	0.65	30	μm^{-1}	[118]	1
Structure and Pertinent length scale of discotic clay gel	P	1.8	0.9	2×10^{-5}	1.5×10^{-4}	Å^{-1}	[119]	1(a)

around $D \cong 1.7$ that corresponds to 2D DLA. In addition, there are some systems with higher dimension, a few of them may correspond to 3D DLA, for which the dimension is $D \cong 2.5$. For porous media we observe a rather flat distribution of fractal dimensions in the range $1.5 < D < 2.8$. For surfaces and fronts there are two peaks, one around $D \cong 1.5$, which includes topologically one-dimensional fronts, and the other one around $D \cong 2.5$, which includes rough two-dimensional surfaces.

The measured dimensions in Table I represent not only empirical measurements of the fractal dimension D_0, but in some cases these are generalized fractal dimensions. In particular, experiments in which scattering techniques are used tend to provide the correlation dimension D_2. The generalized dimension D_q is a monotonically decreasing function of q [122,123].

Due to the broad scope of systems included in our survey, it is not possible at this stage to provide general arguments. We chose to focus our discussion on the class of aggregation systems in which a finite density of DLA-like clusters nucleates on surfaces. These systems are in a way representative,
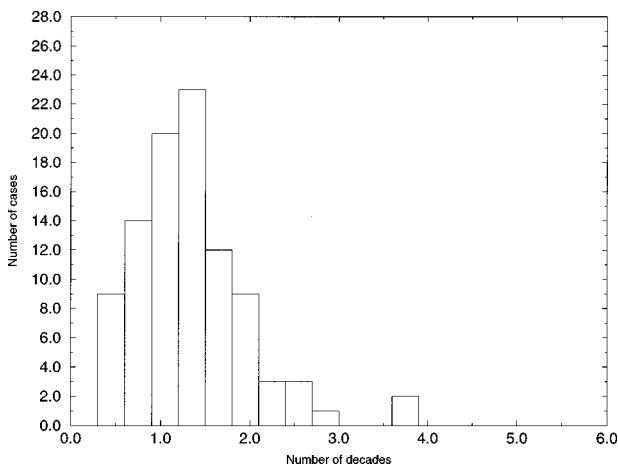

FIG. 1. Distribution of the widths of the scaling range for fractal measurements reported in Physical Review journals between 1990 and 1996. The horizontal axis shows the width of the linear range in the log-log plots (measured in decades) over which the FD was determined and the vertical axis shows the number of measurements in which a given width was obtained. Note that most fractal measurements appear to be based on data that extends between 0.5 and 2 decades. The bin-width is 0.3 decade.

as they exhibit spatial fractal structures that grow out of thermal equilibrium. Moreover, DLA-like structures account for a significant fraction of the surveyed papers and are thus particularly relevant.

III. DLA-LIKE CLUSTERS ON SURFACES

We will now examine the scaling properties and cutoffs in a class of systems in which DLA-like clusters nucleate and grow on a surface. Particularly, in MBE a beam of atoms is deposited on a substrate. These atoms diffuse on the surface and nucleate into islands that keep growing as more atoms are added. MBE experiments on systems such as Au on Ru(0001) [31,124], Cu on Ru(0001) [124], and Pt on Pt(111) [125,126] give rise to DLA like clusters with dimensions close to 1.7. We will now consider the growth processes in such experiments.

In MBE experiments atoms are randomly deposited on a clean high symmetry surface from a beam of flux F [given in monolayers (ML) per second]. Each atom, upon attachment to the surface, starts hopping as a random walker on a lattice [which can be a square lattice for fcc (001) substrates and triangular lattice for fcc (111) substrates] until it either nucleates with other atoms to form an immobile cluster or joins an existing cluster. The hopping rate h_0 (in units of hops per second) for a given atom to each unoccupied nearest neighbor site is

$$h_0 = \nu \exp(-E_0/k_B T), \quad (3.1)$$

where $\nu \cong 10^{12}$ is the standardly used attempt frequency, E_B is the energy barrier, k_B is the Boltzmann factor, and T is the temperature. The coverage after time t is then $\theta = Ft$ (in ML). The submonolayer growth is typically divided into three stages: the early stage is dominated by island nucleation, followed by an aggregation dominated stage until coalescence sets in. In studying the fractal properties of islands we are interested in the late part of the aggregation stage, where islands are already large, but separated from each other, as coalescence is not yet dominant. The scaling behavior at this stage has been studied using both rate equations [127–132] and Monte Carlo (MC) simulations [133–141]. It was found that the density of islands N is given by

$$N \sim \left(\frac{F}{h_0}\right)^{\gamma}. \quad (3.2)$$
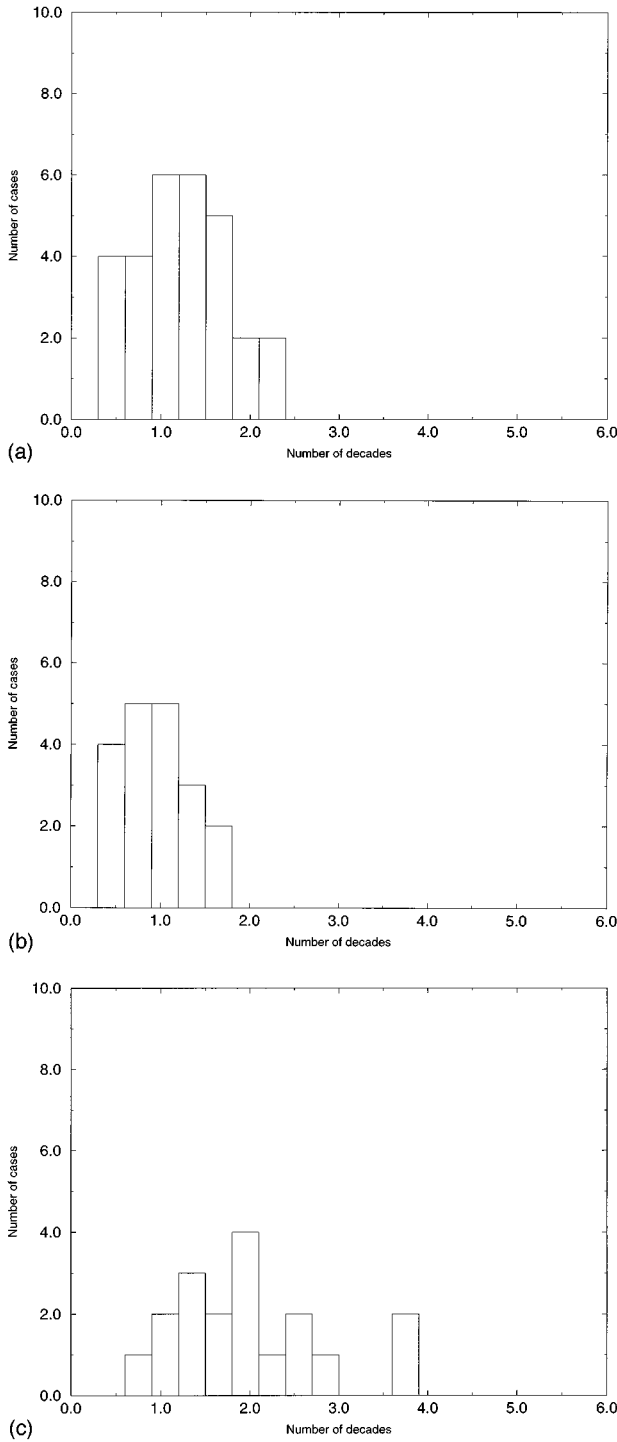
(a)

(b)

(c)

FIG. 2. The distributions of the widths of the scaling range for particular classes of spatial fractals: (a) aggregation, (b) porous media, and (c) surfaces and fronts.

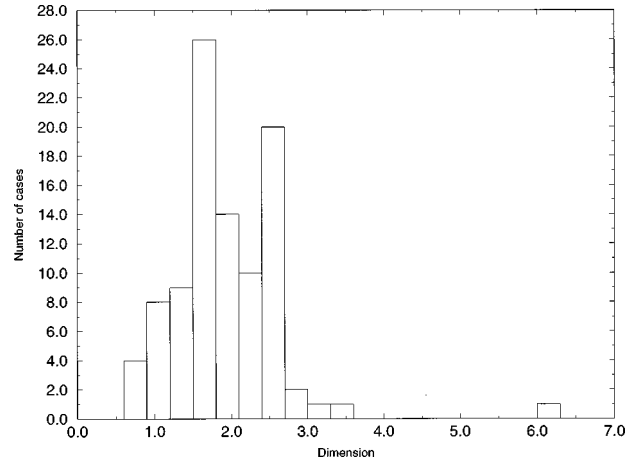FIG. 3. Distribution of experimentally measured fractal dimensions. A broad distribution is observed with peaks around $D=1.7$ and $D=2.5$. The bin width is 0.3.

size $s \leqslant i^*$ are not unstable but only mobile, the scaling exponent takes the form $\gamma = i^*/(2i^*+1)$ [129,141]. For systems in which only the single atom is mobile (such as the DLA model), $i^*=1$ and $\gamma=1/3$ [142]. The typical distance between the centers of islands, which is given by $\ell = N^{-1/2}$, then scales as

$$\ell \sim \left(\frac{h_0}{F}\right)^{1/6}. \tag{3.3}$$

The growth potential of each cluster is limited by this distance, beyond which it merges with its nearest neighbors. Therefore, ℓ is an upper cutoff for the scaling range of the DLA-like islands for the given experimental conditions [143,144]. This cutoff can be pushed up by varying the growth conditions, namely, the temperature and the flux. However, Eq. (3.3) indicates that in order to add one order of magnitude to ℓ one needs to increase the ratio h_0/F by a factor of 10^6. This can be done either by reducing the flux, or by raising the temperature, which would increase the hopping rate. To get a broad scaling range one can also choose a substrate with very low hopping barriers, so the required deposition rate would not have to be unreasonably small. However, the slow dependence of ℓ on h_0/F indicates the inherent difficulties in growing fractal islands with a broad scaling range.

We will now try obtain a more quantitative understanding of the situation. First, we will consider the case of no significant thickening of the arms of the DLA-like clusters. In this case the lower cutoff remains of the order of the atom size. The maximal width of the scaling range is then given by $\Delta_0 = \log_{10}\ell$, where ℓ is given in units of the substrate lattice constant. We thus obtain

$$\Delta_0 = \frac{\gamma}{2}\log_{10}\left(\frac{h_0}{F}\right). \tag{3.4}$$

To approach this width the clusters need to fill the domains of linear size ℓ available to them. The coverage at which this maximal width is obtained is

The exponent γ is determined by the microscopic processes that are activated on the surface during growth. It can be expressed in terms of the critical island size i^*, which is the size for which all islands with a number of atoms $s \leqslant i^*$ are unstable (namely, dissociate after a short time) while islands of size $s \geqslant i^*+1$ are stable. It was found, using scaling arguments and MC simulations that for isotropic diffusion, in the asymptotic limit of slow deposition rate, $\gamma = i^*/(i^*+2)$ [128,137,138]. However, in the case that the small islands of
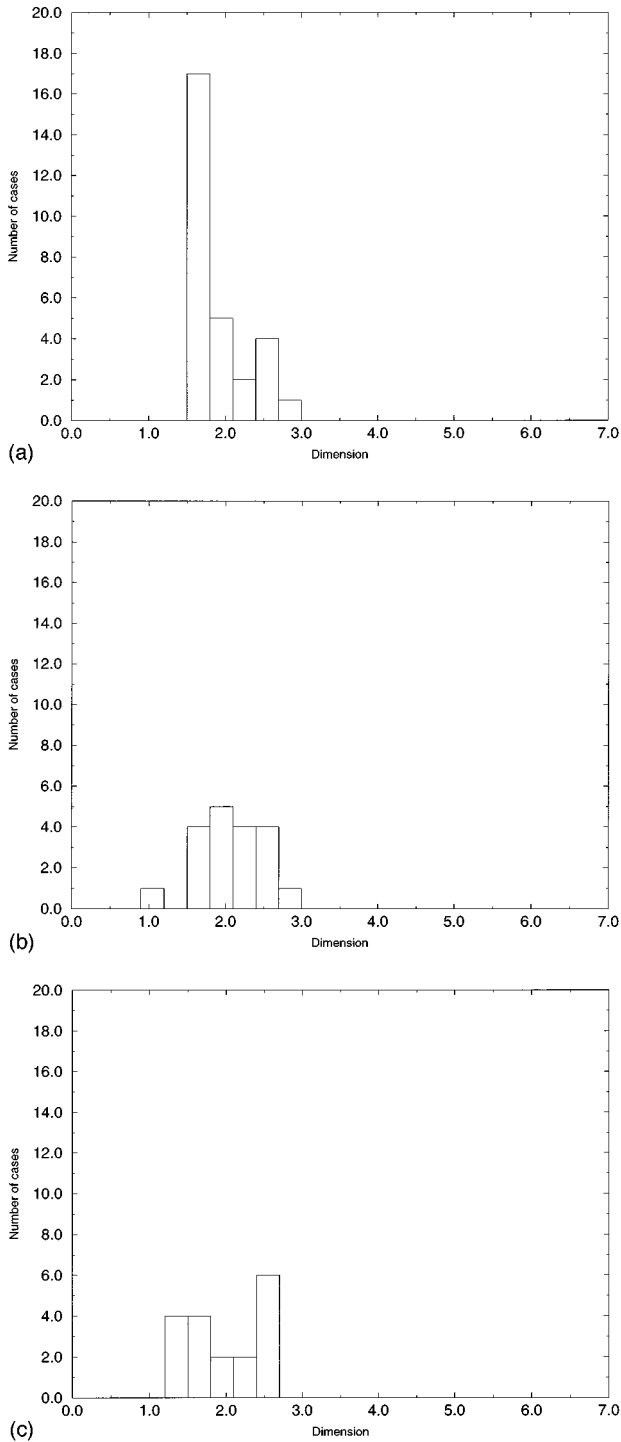
(a)

(b)

(c)

FIG. 4. The distributions of fractal dimensions for particular classes of spatial fractals: (a) aggregation, (b) porous media, and (c) surfaces and fronts.

$$\theta \sim N\ell^D \sim \left(\frac{F}{h_0}\right)^{\gamma(1-D/2)}, \quad (3.5)$$

where D is the FD of the clusters and the deposition time up to this stage is given by $t = \theta/F$. This, together with Eq. (3.4), shows the essential property that a linear increase in the scaling range Δ_0 (given in decades) requires an exponential increase in the duration of the experiment. The dependence of Δ_0 on the hopping energy barrier and the temperature can be obtained from Eq. (3.4) by writing h_0 explicitly from Eq. (3.1), which gives

$$\Delta_0 = \frac{\gamma}{2}\left[\log_{10}\left(\frac{\nu}{F}\right) - \frac{E_0}{k_B T}\log_{10}e\right]. \quad (3.6)$$

It is easy to see that even for a system in which the energy barrier E_0 vanishes, and for the extremely slow deposition rate of $F = 10^{-6}$ ML/s, the width of the scaling range, assuming $\nu = 10^{12}$, would be $\Delta_0 = 3$ decades. Under these conditions, and taking $D = 1.7$, the optimal coverage given by Eq. (3.5) for fractal measurement would be $\theta = 0.126$, which would be obtained after about 35 h of deposition. However, the duration of the deposition experiment in typical submonolayer studies is usually limited to no more than a few hours.

The experimentally feasible scaling range is further limited by the fact that the diffusion properties of physical substrates differ from the DLA model. In particular, the assumption of an infinite separation of time scales, namely, that an isolated atom has high mobility while an atom that has one or more nearest neighbors is completely immobile should be weakened. In a real high symmetry substrate one can identify a variety of hopping rates such as h_0 for an isolated atom, h_{edge} for an atom moving along a step or island edge, and h_{detach} for an atom detaching from a step or island edge. We have seen that for a given substrate temperature, the scaling range can be increased by reducing the flux F. This can be done as long as $h_0 \gg F \gg h_{\text{edge}}, h_{\text{detach}}$. However, once the duration of the experiment (given by $t = \theta/F$) becomes of the order of h_{edge}^{-1} or h_{detach}^{-1}, diffusion along and away from the edges becomes significant and modifies the morphology of the islands. These processes allow atoms to gradually diffuse into the otherwise screened regions of the DLA-like island. As a result, the arms becomes thicker and shorter and the islands become more compact. For the discussion below we will denote by $h_1 = \max(h_{\text{edge}}, h_{\text{detach}})$ the highest hopping rate among the edge moves that may affect the island morphology. h_1 can be expressed in terms of the hopping energy barrier for this process, E_1, just as in Eq. (3.1). The lowest deposition rate that can be used, without having these edge processes affect the morphology, is of the order of $F = h_1$. Using this deposition rate the deposition time up to coverage θ is $t = \theta/h_1$. From Eq. (3.6) and $h_1/\nu = \exp(-E_1/k_B T)$ we obtain that the maximal width Δ of the scaling range, in decades, is then given by

$$\Delta = \frac{\gamma}{2}\left(\frac{E_1 - E_0}{k_B T}\right)\log_{10}e. \quad (3.7)$$

Using Eq. (3.1) one can eliminate the temperature and express this width in terms of the activation energy barriers and the flux F (which is chosen equal to h_1):

$$\Delta = \frac{\gamma}{2}\left(1 - \frac{E_0}{E_1}\right)\log_{10}\left(\frac{\nu}{F}\right). \quad (3.8)$$

To obtain the duration of the deposition experiment, for a given Δ we extract F from Eq. (3.8) and use $t = \theta/F$, where θ is given by Eq. (3.5). We obtain

$$t = \frac{1}{\nu} 10^{K\Delta}, \tag{3.9}$$

where

$$K = \frac{6E_1}{E_1 - E_0} + D - 2. \tag{3.10}$$

This exponential dependence of the experiment duration on Δ clearly limits the feasible scaling range that can be obtained in these experiments. Since $E_1 > E_0$, it is clear that $K \geq 4$. This lower bound is obtained for $E_0 = 0$ and $D = 0$, while typical values for DLA-like clusters are $K \geq 5.7$.

Interestingly, the situation expressed by Eq. (3.9) is somewhat reminiscent of that of the theory of algorithmic complexity [145]. In this theory, there is a distinction between algorithms for which the time complexity function depends polynomially on the input length [typically the number of bits needed to describe the input, i.e., $\sim \ln(\text{input})$], and algorithms for which the dependence is exponential. Generally, problems for which there is a polynomial time algorithm are considered tractable while ones for which there are only exponential time algorithms are considered intractable. One can make a rough analogy between Δ and the input size, and the experimental duration and computation time. Within this analogy, the growth problem considered here, for which the desired large value of Δ is given as input falls, into the class of intractable problems. The understanding of the implications of these ideas to general aggregation problems and other classes of fractal systems would require further studies.

Here we will focus on the conclusions drawn from Eqs. (3.8) and (3.9) on specific experimental systems. fcc (111) metal surfaces are the most promising experimental systems for studies of the growth modes considered here. The energy barriers for Al(111) are $E_0 = 0.04$ eV and $E_1 = 0.32$ eV [146,147]. For Rh(111) $E_0 = 0.16$ eV and $E_1 = 0.54$ eV [148] while for Pt(111) $E_0 = 0.12$ eV and $E_1 = 0.69$ eV [149,150]. These numbers indicate that Al(111) can provide the widest scaling range for an experiment of a given duration. Using the equations above, for Al(111) we find that it is feasible to obtain $\Delta = 2$ decades, which requires $T = 118$ K and $F = 0.02$ ML/s. However, $\Delta = 2.5$ decades is already highly unfeasible since it requires a deposition rate of about 1ML/38 h (at $T = 94$ K). These results seem to be consistent with the experimental findings reported in Sec. II, where for aggregation processes no measurements are reported with significantly more than two decades of scaling range. To summarize, we have shown that the growth of DLA-like clusters is limited by two processes: (1) the nucleation density, and (2) edge mobility and detachment. The resulting clusters can, under realistic conditions, exhibit at most 2–3 decades of scaling range.

IV. DISCUSSION

The MBE systems examined here are representative in the sense that they exhibit spatial fractal structures which form out of thermal equilibrium. The need for a separation of time scales seems to be more general for nonequilibrium aggregation and growth processes, although the details and the particular exponents may be different. Moreover, DLA-like structures account for a significant fraction of the surveyed papers. The analysis presented here is directly relevant to systems in which a finite density of DLA-like clusters is nucleated on a substrate. On the other hand, for growth of a single DLA-like cluster, in problems such as electrodeposition, different considerations are required but we believe that the issue of separation of time scales between the fractal generating processes and the smoothing processes determines the width of the scaling range also there.

To explain why our arguments are specific to nonequilibrium systems we will use 2D percolation as an example of an equilibrium critical system. In a 2D percolation experiment, one can use a similar apparatus as described above for MBE. It is then assumed that diffusion is negligible and atoms are deposited until the coverage reaches the percolation threshold. In such an experiment there is basically no dynamics on the surface. The only constraint is that the deposition will be completed and all measurements are performed at a time scale small compared to the hopping time. However, the hopping time can be made as long as needed by reducing the substrate temperature. Under these conditions, there are no dynamical constraints on the width of the scaling range, which is only limited by the system size, the precision in which the percolation threshold is approached and the apparatus.

The discussion so far focused on highly correlated systems generated by dynamical processes such as diffusion and aggregation. However, weakly correlated systems may also exhibit fractal behavior over a limited range of length scales. This behavior may appear in porous media in the limit of low volume fraction of the pores, or in surface adsorption systems in the low coverage limit. In this case the fractal behavior does not reflect the structure of the basic objects (such as pores or clusters) but their distribution. Using simple models consisting of randomly distributed spherical or rodlike objects, we performed multiple resolution analysis and obtained analytical expression for the box-counting function in this case [151–154]. It was shown that in the uncorrelated case, at subpercolation coverage, one obtains fractal behavior over 0.5–2 decades. The dimensions are found to be nonuniversal, and vary continuously as a function of the coverage. The lower cutoff in these systems is determined by the basic object size while the upper cutoff is given by the average distance between them. It is interesting that this independent analysis, which applies to a different class of systems from the ones we focused on in this paper, also gives rise to a fractal range of less than two decades.

V. SUMMARY

In summary, we have performed a comprehensive survey of experimental papers reporting fractal measurements. Focusing on spatial fractals, these systems were classified according to the types of systems and processes. It was found that for self-similar fractals, the width of the scaling range is typically limited to less than two decades with remarkably few exceptions. In an attempt to examine the origin of this behavior we have focused on a class of MBE experiments in which a finite density of DLA-like clusters nucleate and grow. We have derived an expression of the duration of the

deposition experiment that is required in order to obtain a given width Δ for the scaling range. This expression shows that the experimental time increases exponentially with Δ, given in decades. Applying this expression to real experimental systems, such as the MBE growth of Al on Al(111) it is found that the feasible range is up to about two decades. This result is in agreement with the findings of our survey for aggregation phenomena. Understanding the processes that determine the cutoffs in the entire range of fractal systems, e.g., surfaces and fronts, porous media, and other aggregation processes requires further studies.

ACKNOWLEDGMENTS

[1] B. B. Mandelbrot, *The Fractal Geometry of Nature* (Freeman, San Francisco, 1982).

[2] K. Falconer, *Fractal Geometry: Mathematical Foundations and Applications* (Wiley, Chichester, 1990).

[3] *On Growth and Form*, Vol. 100 in *NATO Advanced Studies Institute Series E: Applied Sciences*, edited by H. E. Stanley and N. Ostrowsky (Martinus Nijhoff, Dordrecht, 1986).

[4] T. Vicsek, *Fractal Growth Phenomena* (World Scientific, Singapore, 1989).

[5] *Fractals in Physics, Essays in Honour of B.B. Mandelbrot*, edited by J. Feder and A. Aharony (North-Holland, Amsterdam, 1990).

[6] H. Takayasu, *Fractals in the Physical Sciences* (J. Wiley & Sons, Chichester, 1990).

[7] *The Fractal Approach to Heterogeneous Chemistry: Surfaces, Colloids, Polymers*, edited by D. Avnir (John Wiley & Sons Ltd., Chichester, 1992).

[8] *Fractals in Science*, edited by A. Bunde and S. Havlin (Springer, Berlin, 1994).

[9] A.-L. Barabási and H.E. Stanley, *Fractal Concepts in Surface Growth* (Cambridge University Press, Cambridge, 1995).

[10] H. E. Stanley, *Introduction to Phase Transitions and Critical Phenomena* (Oxford University Press, Oxford, 1971).

[11] J. J. Binney, N. J. Dowrick, A. J. Fisher, and M. E. J. Newman, *The Theory of Critical Phenomena: An Introduction to the Renormalization Group* (Clarendon Press, Oxford, 1992).

[12] A. Kapitulnik and G. Deutscher, J. Stat. Phys. **36**, 815 (1984).

[13] A. Kapitulnik, Y. Gefen, and A. Aharony, J. Stat. Phys. **36**, 807 (1984).

[14] M. B. Isichenko, Rev. Mod. Phys. **64**, 961 (1992).

[15] D. Stauffer, Phys. Rep. **54**, 1 (1979).

[16] D. Stauffer, *Introduction to Percolation Theory* (Taylor and Francis, London, 1985).

[17] J.-P. Eckmann and D. Ruelle, Rev. Mod. Phys. **57**, 617 (1985).

[18] J. Stavans, F. Heslot, and A. Libchaber, Phys. Rev. Lett. **55**, 596 (1985).

[19] M. H. Jensen, L. P. Kadanoff, A. Libchaber, I. Procaccia, and J. Stavans, Phys. Rev. Lett. **55**, 2798 (1985).

[20] P. Grassberger and I. Procaccia, Physica D **13**, 34 (1984).

[21] J.-P. Eckmann and D. Ruelle, Physica D **56**, 185 (1992).

[22] P. Pfeifer and M. Obert, in *The Fractal Approach to Heterogeneous Chemistry: Surfaces, Colloids, Polymers* (Ref. [7]), p. 11.

[23] T. A. Witten and L. M. Sander, Phys. Rev. Lett. **47**, 1400 (1981).

[24] T. A. Witten and L. M. Sander, Phys. Rev. B **27**, 5686 (1983).

[25] P. Meakin, in *Phase Transitions and Critical Phenomena*, edited by C. Domb and J. L. Lebowitz (Plenum, New York, 1988), Vol. 12, p. 334.

[26] B. B. Mandelbrot, Physica A **191**, 95 (1992).

[27] J.-P. Eckmann, P. Meakin, I. Procaccia, and R. Zeitak, Phys. Rev. Lett. **65**, 52 (1990).

[28] A. Arneodo, F. Argoul, J. F. Muzy, and M. Tabard, Physica A **188**, 217 (1992).

[29] P. Meakin, Phys. Rev. A **27**, 604 (1983).

[30] R. M. Brady and R. C. Ball, Nature (London) **309**, 225 (1984).

[31] R. Q. Hwang, J. Schröder, C. Günter, and R. J. Behm, Phys. Rev. Lett. **67**, 3279 (1991).

[32] Z. R. Struzik, E. H. Dooijes, and F. C. A. Groen, *Fractal Frontiers*, edited by M. M. Novak and T. G. Dewey (World Scientific, Singapore, 1997), p. 189.

[33] The search was done using the command ''find kw fractal or fractals and date 199n and jo physical review and pt experimental'' for $n=0,\ldots,6$. The numbers of papers obtained were 23, 16, 19, 28, 30, 23, and 26 for 1990, ... ,1996, respectively, a total of 165 papers.

[34] J. Liu, W. Y. Shih, M. Sarikaya, and I. A. Aksay, Phys. Rev. A **41**, 3206 (1990).

[35] W.-H. Shih, W. Y. Shih, S.-I. Kim, J. Liu, and I. A. Aksay, Phys. Rev. A **42**, 4772 (1990).

[36] A. Fontana, F. Rocca, M. P. Fontana, B. Rosi, and A. J. Dianoux, Phys. Rev. B **41**, 3778 (1990).

[37] M. Ausloos and P. Clippe, Phys. Rev. B **41**, 9506 (1990).

[38] H. Jian-guo and W. Zi-qin, Phys. Rev. B **42**, 3271 (1990).

[39] F. Devreux, J. P. Boilot, F. Chaput, and B. Sapoval, Phys. Rev. Lett. **65**, 614 (1990).

[40] R. Vacher, E. Courtens, G. Coddens, A. Heidemann, Y. Tsujimi, J. Pelous, and M. Foret, Phys. Rev. Lett. **65**, 1008 (1990).

[41] T. Hwa, E. Kokufuta, and T. Tanaka, Phys. Rev. A **44**, R2235 (1991).

[42] U. Oxaal, Phys. Rev. A **44**, 5038 (1991).

[43] B. X. Liu, C. H. Shang, and H. D. Li, Phys. Rev. B **44**, 4365 (1991).

[44] C. Chachaty, J.-P. Korb, J. R. C. van der Maarel, W. Bras, and P. Quinn, Phys. Rev. B **44**, 4778 (1991).

[45] C. H. Shang, B. X. Liu, J. G. Sun, and H. D. Li, Phys. Rev. B **44**, 5035 (1991).

[46] A. Birovljev, L. Furuberg, J. Feder, T. Jøssang, K. Måløy, and A. Aharony, Phys. Rev. Lett. **67**, 584 (1991).

[47] P. Constantin, I. Procaccia, and K. R. Sreenivasan, Phys. Rev. Lett. **67**, 1739 (1991).

[48] E. Lemaire, P. Levitz, G. Daccord, and H. Van Damme, Phys. Rev. Lett. **67**, 2009 (1991).

[49] R. Q. Hwang, J. Schröder, C. Günther, and R. J. Behm, Phys. Rev. Lett. **67**, 3279 (1991).

[50] M. Adam, D. Lairez, F. Boué, J. P. Busnel, D. Durand, and T. Nicolai, Phys. Rev. Lett. **67**, 3456 (1991).

[51] F. Ferri, B. J. Frisken, and D. S. Cannell, Phys. Rev. Lett. **67**, 3626 (1991).

[52] D. Asnaghi, M. Carpineti, M. Giglio, and M. Sozzi, Phys. Rev. A **45**, 1018 (1992).

[53] D. J. Robinson and J. C. Earnshaw, Phys. Rev. A **46**, 2045 (1992).

[54] D. J. Robinson and J. C. Earnshaw, Phys. Rev. A **46**, 2065 (1992).

[55] P. McAnulty, L. V. Meisel, and P. J. Cote, Phys. Rev. A **46**, 3523 (1992).

[56] A. Sánchez, R. Serna, F. Catalina, and C. N. Afonso, Phys. Rev. B **46**, 487 (1992).

[57] D. Ghosh, P. Ghosh, A. Deb, D. Halder, S. Das, A. Hossain, A. Dey, and J. Roy, Phys. Rev. D **46**, 3712 (1992).

[58] M. Carpineti and M. Giglio, Phys. Rev. Lett. **68**, 3327 (1992).

[59] D. K. Schwartz, S. Steinberg, J. Israelachvili, and J. A. N. Zasadzinski, Phys. Rev. Lett. **69**, 3354 (1992).

[60] P. Jensen, P. Melinon, M. Treilleux, J. X. Hu, J. Dumas, A. Hoareau, and B. Cabaud, Phys. Rev. B **47**, 5008 (1993).

[61] Z. Q. Mu, C. W. Lung, Y. Kang, and Q. Y. Long, Phys. Rev. B **48**, 7679 (1993).

[62] H. Iwasaki and T. Yoshinobu, Phys. Rev. B **48**, 8282 (1993).

[63] J. Zhang, D. Liu, and K. Colbow, Phys. Rev. B **48**, 9130 (1993).

[64] A. Hasmy, M. Foret, J. Pelous, and R. Jullien, Phys. Rev. B **48**, 9345 (1993).

[65] G. P. Luo, Z. M. Ai, J. J. Hawkes, Z. H. Lu, and Y. Wei, Phys. Rev. B **48**, 15 337 (1993).

[66] K. Sengupta, M. L. Cherry, W. V. Jones, J. P. Wefel, A. Dabrowska, R. Holyński, A. Jurak, A. Olszewski, M. Szarska, A. Trzupek, B. Wilczyńska, H. Wilczyński, W. Wolter, B. Wosiek, K. Woźniak, P. S. Freier, and C. J. Waddington, Phys. Rev. D **48**, 3174 (1993).

[67] T. Buzug, J. von Stamm, and G. Pfister, Phys. Rev. E **47**, 1054 (1993).

[68] J. Stankiewicz, M. A. C. Vilchez, and R. H. Alvarez, Phys. Rev. E **47**, 2663 (1993).

[69] N. Ming, M. Wang, and R.-W. Peng, Phys. Rev. E **48**, 621 (1993).

[70] P. Carro, S. L. Marchiano, A. H. Creus, S. González, R. C. Salvarezza, and A. J. Arvia, Phys. Rev. E **48**, R2374 (1993).

[71] Q. Wei, X. Liu, C. Zhou, and N. Ming, Phys. Rev. E **48**, 2786 (1993).

[72] B. Sapoval, R. Gutfraind, P. Meakin, M. Keddam, H. Takenouti, Phys. Rev. E **48**, 3333 (1993).

[73] M. Sahimi, M. C. Robertson, and C. G. Sammis, Phys. Rev. Lett. **70**, 2186 (1993).

[74] J. H. Page, J. Liu, B. Abeles, H. W. Deckman, and D. A. Weitz, Phys. Rev. Lett. **71**, 1216 (1993).

[75] J. C. Li, D. K. Ross, L. D. Howe, K. L. Stefanopoulos, J. P. A. Fairclough, R. Heenan, and K. Ibel, Phys. Rev. B **49**, 5911 (1994).

[76] S. Sen and J. F. Stebbins, Phys. Rev. B **50**, 822 (1994).

[77] R. Xie, B. Yang, and B. Jiang, Phys. Rev. B **50**, 3636 (1994).

[78] A. Hasmy, E. Anglaret, M. Foret, J. Pelous, and R. Jullien, Phys. Rev. B **50**, 6006 (1994).

[79] T. Ohsaka and T. Ihara, Phys. Rev. B **50**, 9569 (1994).

[80] J. C. Groote, J. R. W. Weerkamp, J. Seinen, and H. W. den Hartog, Phys. Rev. B **50**, 9798 (1994).

[81] D. Ghosh, A. Deb, M. Lahiri, A. Dey, S. A. Hossain, S. Das, S. Sen, and S. Halder, Phys. Rev. D **49**, 3113 (1994).

[82] W. Shaoshun, Z. Jie, Y. Yunxiu, X. Chenguo, and Z. Yu, Phys. Rev. D **49**, 5785 (1994).

[83] R. K. Shivpuri and V. Anand, Phys. Rev. D **50**, 287 (1994).

[84] L. Vázquez, R. C. Salvarezza, P. Ocón, P. Herrasti, J. M. Vara, and A. J. Arvia, Phys. Rev. E **49**, 1507 (1994).

[85] Q. Wei, M. Han, C. Zhou, and N. Ming, Phys. Rev. E **49**, 4167 (1994).

[86] V. Panella and J. Krim, Phys. Rev. E **49**, 4179 (1994).

[87] A. Birovljev, K. J. Måløy, J. Feder, and T. Jøssang, Phys. Rev. E **49**, 5431 (1994).

[88] Y. Xiao, Phys. Rev. E **49**, 5903 (1994).

[89] C. D. Muzny, G. C. Straty, and H. J. M. Hanley, Phys. Rev. E **50**, R675 (1994).

[90] T. Holten, T. Jøssang, P. Meakin, and J. Feder, Phys. Rev. E **50**, 754 (1994).

[91] P. W. Zhu and D. H. Napper, Phys. Rev. E **50**, 1360 (1994).

[92] J. Cai and C. M. Sorensen, Phys. Rev. E **50**, 3397 (1994).

[93] E. K. Hobbie, B. J. Bauer, and C. C. Han, Phys. Rev. Lett. **72**, 1830 (1994).

[94] A. Komori, T. Baba, T. Morisaki, M. Kono, H. Iguchi, K. Nishimura, H. Yamada, S. Okamura, and K. Matsuoka, Phys. Rev. Lett. **73**, 660 (1994).

[95] M. S. Spector, E. Naranjo, S. Chiruvolu, and J. A. Zasadzinski, Phys. Rev. Lett. **73**, 2867 (1994).

[96] A. Kuhn, F. Argoul, J. F. Muzy, and A. Arneodo, Phys. Rev. Lett. **73**, 2998 (1994).

[97] M. Ivanda, I. Hartmann, and W. Kiefer, Phys. Rev. B **51**, 1567 (1995).

[98] S. J. Sze and T. Y. Lee, Phys. Rev. B **51**, 8709 (1995).

[99] C. Douketis, Z. Wang, T. L. Haslett, and M. Moskovits, Phys. Rev. B **51**, 11 022 (1995).

[100] A. C. Mitropoulos, J. M. Haynes, and R. M. Richardson, Phys. Rev. B **52**, 10 035 (1995).

[101] R. K. Shivpuri, G. Das, and S. Dheer, Phys. Rev. C **51**, 1367 (1995).

[102] S. Dheer, G. Das, R. K. Shivpuri, and S. K. Soni, Phys. Rev. C **52**, 1572 (1995).

[103] T. Abbott *et al.*, Phys. Rev. C **52**, 2663 (1995).

[104] D. Ghosh, A. Deb, and M. Lahiri, Phys. Rev. D **51**, 3298 (1995).

[105] A. E. Larsen, D. G. Grier, and T. C. Halsey, Phys. Rev. E **52**, R2161 (1995).

[106] A. Arneodo, E. Bacry, P. V. Graves, and J. F. Muzy, Phys. Rev. Lett. **74**, 3293 (1995).

[107] R. Viswanathan, and M. B. Heaney, Phys. Rev. Lett. **75**, 4433 (1995).

[108] Y. L. Wang and S. J. Lin, Phys. Rev. B **53**, 6152 (1996).

[109] C. H. Shang, Phys. Rev. B **53**, 13 759 (1996).

[110] A. P. Radlinski and C. J. Boreham, Phys. Rev. B **53**, 14 152 (1996).

[111] M. S. Mattsson, G. A. Niklasson, and C. G. Granqvist, Phys. Rev. B **54**, 2968 (1996).

[112] M. S. Mattsson, G. A. Niklasson, and C. G. Granqvist, Phys. Rev. B **54**, 17 884 (1996).

[113] M. L. Cherry *et al.*, Phys. Rev. C **53**, 1532 (1996).

[114] R. Du and H. A. Stone, Phys. Rev. E **53**, 1994 (1996).

[115] L. Balazs, V. Fleury, F. Duclos, and A. Van Herpen, Phys. Rev. E **54**, 599 (1996).

[116] H.-P. Muller, R. Kimmich, and J. Weis, Phys. Rev. E **54**, 5278 (1996).

[117] U. Bisang and J. H. Bilgram, Phys. Rev. E **54**, 5309 (1996).

[118] F. Mallamace, N. Micali, S. Trusso, L. M. Scolaro, A. Romeo, A. Terracina, and R. F. Pasternack, Phys. Rev. Lett. **76**, 4741 (1996).

[119] F. Pignon, J. M. Piau, and A. Magnin, Phys. Rev. Lett. **76**, 4857 (1996).

[120] Conventionally, log of base 10 is used for both horizontal and vertical axes and the width of the linear range is given in decades. In cases where a different base was used we converted it to base 10. It is also important to realize that the property presented in the horizontal axis should have a linear dimension (such as length, time, etc.) as fractal dimension relates some generalized volume to a linear stick size. If the feature presented has dimensions of area, for example, the apparent width of the linear range will double. In a number of cases we had to correct the width measurements to avoid such effects.

[121] The only paper reporting a dimension much larger than 3 is Ref. [94] where the fractal dimension of a strange attractor in turbulent plasma was measured.

[122] H. G. E. Hentschel and I. Procaccia, Physica D **8**, 435 (1983).

[123] T. C. Halsey, M. H. Jensen, L. P. Kadanoff, I. Procaccia, and B. Shraiman, Phys. Rev. A **33**, 1141 (1986).

[124] G. Potschke, J. Schroder, C. Gunther, R. Q. Hwang, and R. J. Behm, Surf. Sci. **251**, 592 (1991).

[125] M. Bott, T. Michely, and G. Comsa, Surf. Sci. **272**, 161 (1992).

[126] T. Michely, M. Hohage, M. Bott, and G. Comsa, Phys. Rev. Lett. **70**, 3943 (1993).

[127] S. Stoyanov and D. Kashchiev, Curr. Top. Mater. Sci. **7**, 70 (1981).

[128] J. A. Venables, G. D. T. Spiller, and M. Hanbucken, Rep. Prog. Phys. **47**, 399 (1984).

[129] J. Villain, A. Pimpinelli, and D. Wolf, Comments Condens. Matter Phys. **16**, 1 (1992); J. Villain, A. Pimpinelli, L. Tang, and D. Wolf, J. Phys. I **2**, 2107 (1992).

[130] M. C. Bartelt and J. W. Evans, Phys. Rev. B **46**, 12 675 (1992); M. C. Bartelt, M. C. Tringides, and J. W. Evans, *ibid.* **47**, 13 891 (1993).

[131] L. Tang, J. Phys. I **3**, 935 (1993).

[132] O. Biham, G. T. Barkema, and M. Breeman, Surf. Sci. **324**, 47 (1995).

[133] C. Ratsch, A. Zangwill, P. Smilauer, and D. D. Vvedensky, Phys. Rev. Lett. **72**, 3194 (1994); C. Ratsch, P. Smilauer, A. Zangwill, and D. D. Vvedensky, Surf. Sci. **329**, L599 (1995).

[134] Z. Zhang, X. Chen, and M. G. Lagally, Phys. Rev. Lett. **73**, 1829 (1994).

[135] J. Jacobsen, K. W. Jacobsen, P. Stoltze, and J. K. Norskov, Phys. Rev. Lett. **74**, 2295 (1994).

[136] G. T. Barkema, O. Biham, M. Breeman, D. O. Boerma, and G. Vidali, Surf. Sci. Lett. **306**, L569 (1994).

[137] M. Schroeder and D. E. Wolf, Phys. Rev. Lett. **74**, 2062 (1995); D. E. Wolf, in *Scale Invariance, Interfaces, and Non-Equilibrium Dynamics*, edited by M. Droz, A. J. McKane, J. Vannimenus, and D. E. Wolf, Vol. 344 of *NATO Advanced Studies Institutes Series B: Physics* (Plenum, New York, 1994).

[138] J. G. Amar and F. Family, Phys. Rev. Lett. **74**, 2066 (1995); Thin Solid Films **272**, 208 (1996); F. Family and J. G. Amar, Mater. Sci. Eng. B **30**, 149 (1995).

[139] G. S. Bales and D. C. Chrzan, Phys. Rev. Lett. **74**, 4879 (1995).

[140] T. R. Linderoth, J. J. Mortensen, K. W. Jacobsen, E. Laegsgaard, I. Stensgaard, and F. Besenbacher, Phys. Rev. Lett. **77**, 87 (1996).

[141] I. Furman and O. Biham, Phys. Rev. B **55**, 7917 (1997).

[142] In the present analysis we focus on the case $i^*=1$ and $\gamma=1/3$. In systems for which $\gamma \neq 1/3$ there are unstable or mobile islands of size $s \geq 2$. Such systems exhibit mobility along island edges or detachment moves that modify the morphology from fractal to more compact even at the time scale of single atom hopping, and therefore are not relevant for our considerations.

[143] In principle, one can vary the deposition rate during the growth process. This is typically used to increase the number of nucleation sites, which is helpful for epitaxial growth [144]. This is achieved by starting with a high deposition rate and gradually reducing it as the coverage increases. The large number of islands nucleated in the early stages are stable and keep aggregating more atoms in spite of the reduced deposition rate. For the purpose of growing larger DLA-like islands in a shorter time one may want to use a slow deposition rate in the early stages and increase it gradually. However, in this case new islands will continue to nucleate and the low island density of the initial low deposition rate will not be maintained.

[144] G. Rosenfeld, R. Servaty, C. Teichert, B. Poelsma, and G. Comsa, Phys. Rev. Lett. **71**, 895 (1993).

[145] M. R. Garey and D. S. Johnson, *Computers and Intractability: A Guide to the Theory of NP-Completeness* (Freeman, New York, 1979).

[146] R. Stumpf and M. Scheffler, Phys. Rev. Lett. **72**, 254 (1994).

[147] R. Stumpf and M. Scheffler, Phys. Rev. B **53**, 4958 (1996).

[148] G. Ayrault and G. Ehrlich, J. Chem. Phys. **60**, 281 (1974).

[149] D. W. Basset and P. R. Webber, Surf. Sci. **70**, 520 (1978).

[150] D. W. Basset and P. R. Webber, Surf. Sci. **246**, 31 (1991).

[151] D. A. Hamburger, O. Malcai, O. Biham, and D. Avnir, in *Fractals and Chaos in Chemical Engineering* (World Scientific, Singapore, 1997).

[152] D. A. Hamburger, O. Biham, and D. Avnir, Phys. Rev. E **53**, 3342 (1996).

[153] D. A. Lidar (Hamburger), O. Biham and D. Avnir, J. Chem. Phys. **106**, 10 359 (1997).

[154] D. Avnir, O. Biham, D. A. Lidar (Hamburger), and O. Malcai, in *Fractal Frontiers*, edited by M. M. Novak and T. G. Dewey (World Scientific, Singapore, 1997), p. 199.